JOURNAL OF APPLIED POLYMER SCIENCE VOL. 20, 501–523 (1976)

The Influence of Titanium Dioxide on the Rheological and Extrusion Properties of Polymer Melts

NOBUHIKO MINAGAWA* and JAMES L. WHITE, *Department of Chemical and Metallurgical Engineering, The University of Tennessee, Knoxville, Tennessee 37916*

Synopsis

An experimental study of the influence of titanium dioxide (TiO_2) on the rheological and extrusion properties of five polymer melts (two low-density polyethylenes, two high-density polyethylenes, and a polystyrene) has been carried out. Increasing TiO_2 loading increases the shear viscosity η, with the extent of increase being greater at lower shear rates. At moderate and high TiO_2 loadings, the filled melts may possess yield values. Empirical equations relating viscosity to filler loading have been developed. The first normal stress difference was measured for the melts and found to increase with increasing TiO_2 loading. However, the extent of increase was less than found for the viscosity function and interpretation in terms of the theory of viscoelasticity suggests that the characteristic relaxation time of the melts decreases with increasing TiO_2 level. Empirical equations relating the first normal stress difference coefficient to volume fraction of the filler have been developed. Addition of TiO_2 is found to decrease extrudate swell and retard the occurrence of extrudate distortion.

INTRODUCTION

The influence of solid fillers on the rheological properties of molten polymers is both of great scientific interest and has important industrial applications. Fillers are added to polymers for such diverse purposes as providing reinforcement for mechanical properties, to provide optical covering character (opacity). In this paper, we will consider the influence of titanium dioxide (TiO_2) fillers on the rheological and extrusion properties of a series of polymer melts. TiO_2 is an important industrial pigment additive because it provides a high level of hiding power, gloss, and brightness at low loading levels.[1–3]

Previous studies of the influence of fillers on flow properties of polymer melts may be divided into the investigation of (1) shear viscosity, (2) viscoelastic properties, and (3) extrusion characteristics. There have been numerous studies of the influence of filler on the viscosity function of polymer melts and solutions. Most of these studies have been with carbon black and rubber,[4–12] but a limited number of studies have appeared on other fillers such as calcium silicate,[13] magnesium silicate,[14] calcium carbonate,[15] crosslinked glassy polymer beads,[13,16] and inorganic glass beads[17–20] in polymer melts and solutions. Generally, fillers increase the level of the viscosity, but the extent

*Permanent address: Fuji Photo Film Company, Ltd., Fujinomiya, Shizuoka, Japan.

TABLE I
Description of Polymers

Symbol	Material	Commercial description	Melt index
HDPE-0.1	high-density polyethylene	Phillips Petroleum, EHM-6001	0.1
HDPE-5	high-density polyethylene	Phillips Petroleum, EMB-6050	5.0
LDPE-5	low-density polyethylene	Dow Chemical, 610M	5.0
LDPE-23	low-density polyethylene	Union Carbide, DNDA-0917	23
PS	polystyrene	Dow Chemical, Styron-678	—

seems to vary from system to system and to decrease with increasing shear rate.

There have been a limited number of studies of viscoelastic properties of polymer melts and solutions containing fillers[11,16,21–24] which consider the effects on the relaxation spectrum. The studies of Onogi et al. are especially noteworthy. With the possible exception of Han's study[15] of calcium carbonate-filled polypropylene, there have been no studies at normal stresses in filled polymer systems. Various researchers have studied the influence of carbon black on the extrusion characteristics of rubber,[5,7,11,12] finding that black surface area and structure decrease extrudate swell and retard the development of extrudate distortion. There seem to be no previous studies of the influence of TiO_2 on the rheological and extrusion properties of polymer melts.

EXPERIMENTAL

Material

Five commercial polymers were included in this study. These were two high-density polyethylenes with melt indices 0.1 and 5.0, two low-density polyethylenes with melt indices 5.0 and 23, and a polystyrene. These materials, which we have designated in the remainder of this paper HDPE-0.1, HDPE-5, LDPE-5, LDPE-23, and PS, are summarized in Table I.

Three commercial TiO_2 pigments supplied by E. I. du Pont de Nemours were studied. The particle sizes were in the range of 0.18–0.25 microns. The characteristics of the three TiO_2 pigments are summarized in Table II.

Mixing

The TiO_2 pigments were blended into the polymer melts using a two-roll laboratory mill at 140°C. Blends with TiO_2 contents ranging from 5 to 40 vol-% (based upon 20°C densities) were prepared. Small amounts of antioxidant (Irganox-1010) and a wetting agent (calcium stearate) were added during mixing.

The TiO_2 compounds were compared to unfilled polymer melts which had been masticated under equivalent conditions. Identical amounts of antioxidant and wetting agent (calcium stearate) were added to these polymers.

Rheological Property Measurement

In a laminar shearing flow, i.e., where the velocity field has the form

$$v_1 = v_1(x_2),\ v_2 = v_3 = 0 \tag{1}$$

TABLE II
Description of Titanium Dioxides Studied

Symbol	Commercial description	Particle size, μ	TiO_2%	Modification
TiO_2-A	du Pont, R-101	0.18	97	Al_2O_3
TiO_2-B	du Pont, R-100	0.24	97	Al_2O_3
TiO_2-C	du Pont, R-902	0.25	90	Al_2O_3, SiO_2

the stress tensor in a viscoelastic fluid may be expressed as follows:

$$\begin{vmatrix} \sigma_{11} & \sigma_{12} & \sigma_{13} \\ \sigma_{12} & \sigma_{22} & \sigma_{23} \\ \sigma_{13} & \sigma_{23} & \sigma_{33} \end{vmatrix} = - \begin{vmatrix} p & 0 & 0 \\ 0 & p & 0 \\ 0 & 0 & p \end{vmatrix} + \begin{vmatrix} \beta_1\dot{\gamma}^2 & \eta\dot{\gamma} & 0 \\ \eta\dot{\gamma} & \beta_2\dot{\gamma}^2 & 0 \\ 0 & 0 & 0 \end{vmatrix} \tag{2}$$

Generally, three rheological functions, a viscosity η and two normal stress difference coefficients Ψ_1 and Ψ_2 defined by

$$\eta = \sigma_{12}/\dot{\gamma} \tag{3a}$$

$$\Psi_1 = \beta_1 - \beta_2 = (\sigma_{11} - \sigma_{22})/\dot{\gamma}^2 = N_1/\dot{\gamma}^2 \tag{3b}$$

$$\Psi_2 = \beta_2 = (\sigma_{22} - \sigma_{33})/\dot{\gamma}^2 = N_2/\dot{\gamma}^2 \tag{3c}$$

are measured. While numerous measurements of the viscosity for polymer melts have appeared and several of Ψ_1, there have been very few of Ψ_2.[26–31] However, it is clear that Ψ_2 is much smaller, in general, than Ψ_1 and is usually negative.[28,31]

In our studies, we have measured the viscosity $\eta(\dot{\gamma})$ using both a Weissenberg rheogoniometer and an Instron capillary rheometer. The first normal stress difference N_1 was measured by a Weissenberg rheogoniometer. All measurements were performed at 180°C.

In our rheogoniometer studies, the shear rate was determined through the relation[32,33]

$$\dot{\gamma} = \frac{\Omega}{\psi} \tag{4}$$

where Ω is the rotation rate and ψ is the angle between the cone and plate. The shear stress σ_{12} was obtained from torque measurements[32,33] through

$$\sigma_{12} = \frac{3T}{2\pi R^3} \tag{5}$$

where T is the torque applied and R is the radius of cone and plate. The viscosity $\eta(\dot{\gamma})$ was obtained from the ratio of eq. (5) to eq. (4). The first normal stress difference N_1 was obtained from total thrust F measurements with the expression[32,33]

$$N_1 = \frac{2F}{\pi R^2} \tag{6}$$

TABLE III
Filled Polymers Prepared

Polymers	TiO_2 Loadings		
	Weight, %	Volume (20°C), %	Volume (180°C), %
HDPE-0.1 and HDPE-5	0	0	0
	18.7	5.0	4.2
	43.4	15.0	12.7
	59.3	25.0	21.6
	74.5	40.0	35.5
LDPE-5 and LDPE-23	0	0	0
	19.4	5.0	4.3
	44.6	15.0	13.0
	60.3	25.0	22.1
	75.3	40.0	36.0
PS	0	0	0
	17.8	5.0	4.8
	42.1	15.0	14.3
	58.0	25.0	24.0
	73.2	40.0	38.6

and Ψ_1 was determined using eqs. (3b), (4), and (6). In our studies, a 2.5-cm diameter cone and 4° cone angle were used. Rheogoniometer measurements were limited to low shear rate range of order 1 sec^{-1} and below because of flow instability of polymer flow between cone and plate. These have also been reported by other authors.[27,29,31]

In the capillary rheometer, shear rates were determined at the capillary wall through the expression[33,34]

$$\dot{\gamma}_w = \left(-\frac{dv_1}{dr}\right)_w = \left(\frac{3n'+1}{4n'}\right)\frac{32Q}{\pi D^3} = \left(\frac{3n'+1}{4n'}\right)\frac{8V}{D} \tag{7a}$$

$$n' = \frac{d \log D\Delta p_c/4L}{d \log 32Q/\pi D^3} \tag{7b}$$

where D is capillary diameter, L is the length, Q is the volumetric extrusion rate, v_1 is the linear velocity, v is the average velocity, Δp_c is the pressure drop within the capillary, and r is the radius variable. The shear stress was obtained by plotting total pressure loss versus die L/D ratio and determining the slope.[35,29] In particular, we used the expression

$$p = \Delta p_e + \Delta p_c = \Delta p_e + 4(\sigma_{12})_w \cdot \frac{L}{D} \tag{8}$$

where Δp_e is the sum of the pressure loss at the entrance and exit of the capillary, and $(\sigma_{12})_w$ is the shear stress at the capillary wall. Three capillary dies with diameter of from 0.052 to 0.054 in. and L/D ratio of 5, 9, and 28 were used.

Extrusion Experiments

Studies of the extrusion of TiO_2–polymer melt compounds were carried out in an Instron capillary rheometer using the capillary dies described in the previous section. Special attention was given to extrudate quality, especially

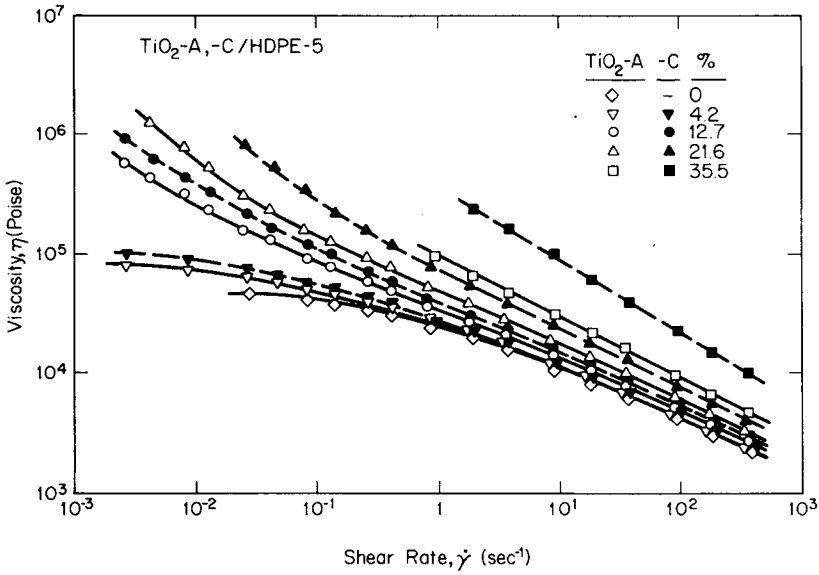

Fig. 1. Viscosity–shear rate behavior of HDPE-5 with various levels of TiO_2-A and TiO_2-C at 180°C.

the magnitude of extrudate swell and the smoothness of the surface or occurrence of distortion. Extrudate swell was measured in two manners. First, the diameters of the frozen extrudates, in other words, the extrudates solidified at room temperature, were measured and compared with capillary diameter. In a second series of experiments, the extrudates were stress relieved by heating them in hot silicone oil of 160°C, similar to the manner suggested by Nakajima and Shida[36] and others.[37,38,39]

We also considered the magnitude of the entrance pressure loss. Specifically, as we may write in eq. (8)

$$p = 4(\sigma_{12})_w \left[\frac{L}{D} + \left(\frac{1}{4}\right)\frac{\Delta p_e}{(\sigma_{12})_w}\right]. \tag{9}$$

The ratio $\Delta p_e/(\sigma_{12})_w$ represents an effective increase in capillary L/D ratio. Various researchers have also considered Δp_e or this ratio to possess rheological significance.[40–42,29]

RHEOLOGICAL PROPERTIES

Viscosity Results

The viscosity–shear rate relationship for the HDPE-0.1, HDPE-5, LDPE-5, LDPE-23, and PS with various loadings of TiO_2 is shown in Figures 1–5. A study of the literature on the hydrodynamics of suspensions[43,44] suggests that a proper means of comparison is to represent the viscosity as a function of the volume fraction of suspended particles. The volume fraction ϕ is related to the weight fraction w_{TiO_2} through the expression

$$\phi = \frac{w_{TiO_2}/\rho_{TiO_2}}{(w_{TiO_2}/\rho_{TiO_2}) + ([1 - w_{TiO_2}]/\rho_{polymer})}. \tag{10}$$

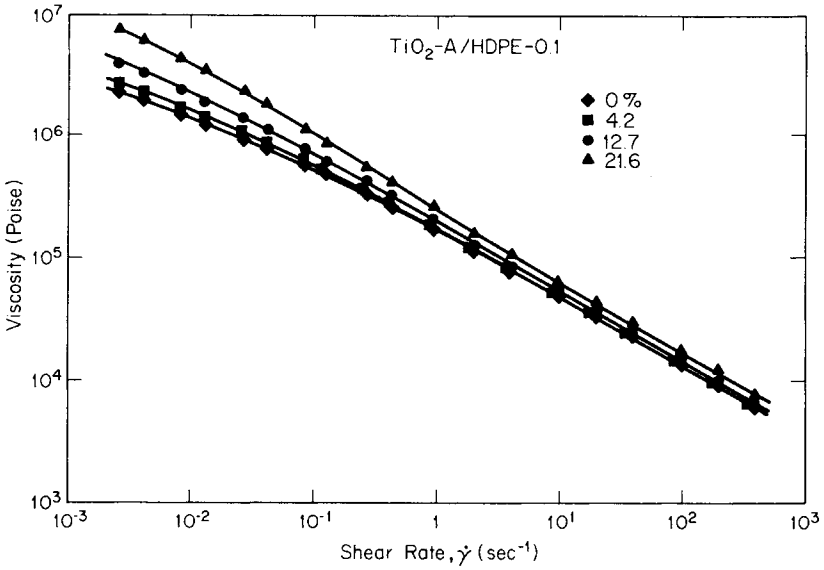

Fig. 2. Viscosity–shear rate behavior of HDPE-0.1 with various levels of TiO_2-A at 180°C.

The question of the material densities ρ_{TiO_2} and $\rho_{polymer}$ must be considered. The proper comparison involves using densities at the temperature the measurements were made, i.e., 180°C. We have used 4.1 for TiO_2, 0.77 for the polyethylenes, 0.96 for polystyrene. Table III summarizes the volume and weight fractions studied in the different melts.

It may be seen in Figures 1–5 that the viscosity $\eta(\phi,\dot{\gamma})$ is a decreasing function of shear rate and an increasing function of the filler loading at any shear rate. The magnitude of the viscosity increase is a strong function of shear rate, with the increase being substantially greater in the low shear rate range.

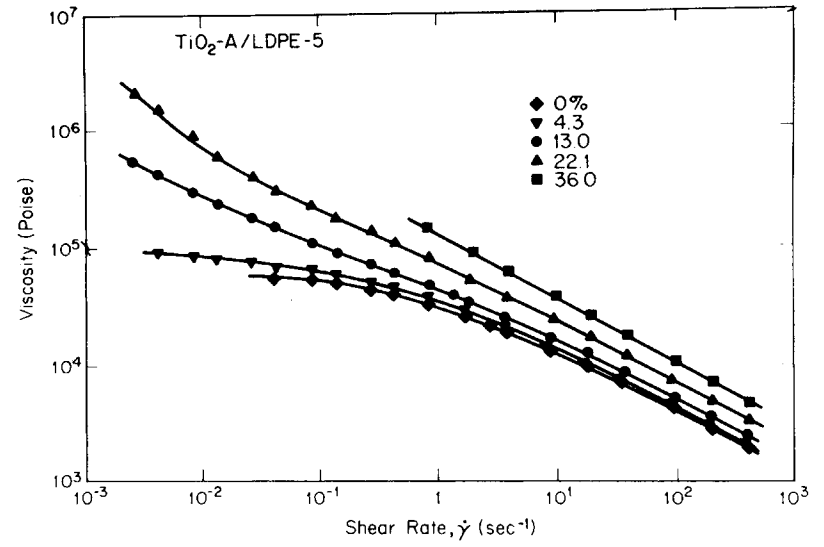

Fig. 3. Viscosity–shear rate behavior of LDPE-5 with various levels of TiO_2-A at 180°C.

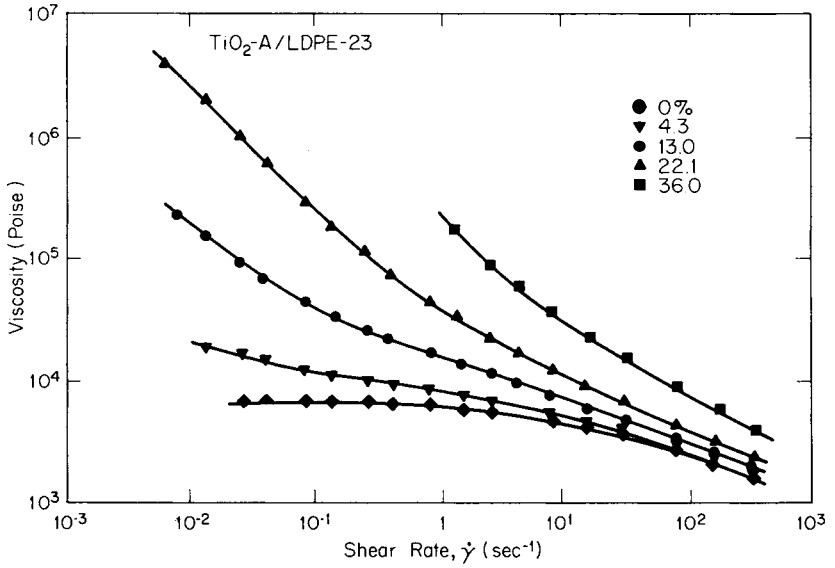

Fig. 4. Viscosity–shear rate behavior of LDPE-23 with various levels of TiO_2-A at 180°C.

The effect may be strikingly seen in Figure 6, where the relative viscosity $\eta(\phi)/\eta(0)$ is replotted from Figure 1 for TiO_2-A in HDPE-5. There would seem a trend toward the suspension having a yield value.

The relative influence of TiO_2-A on the five polymers under study is shown in Figure 7. The effect is greatest for the LDPE-23 and the following orders:

LDPE-23 > LDPE-5 > HDPE-5 > PS > HDPE-0.1.

The influence of the type of TiO_2 on melt viscosity is brought out in Figure

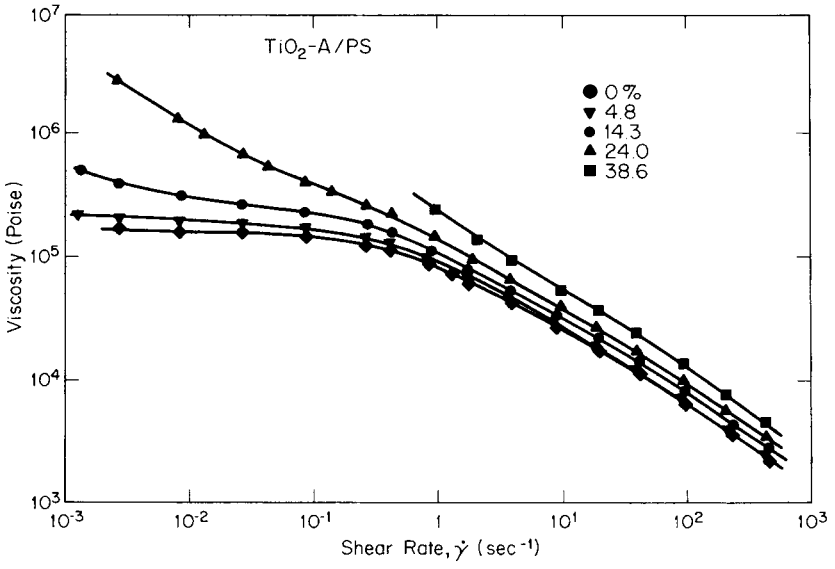

Fig. 5. Viscosity–shear rate behavior of PS with various levels of TiO_2-A at 180°C.

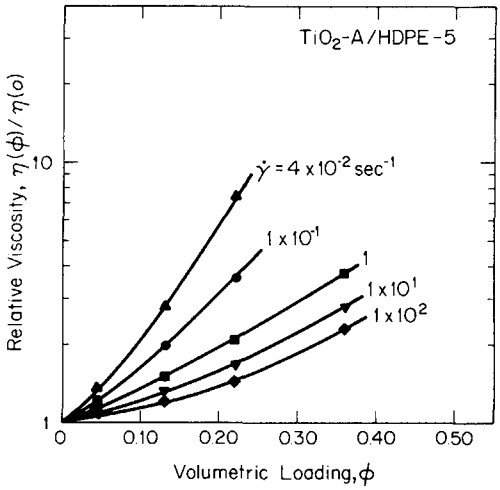

Fig. 6. Relative viscosity $\eta(\phi)/\eta(0)$ as a function of volumetric loading ϕ for HDPE-5 with TiO_2-A.

8. The influences of types A and B are similar, and type C causes greater increases in viscosity.

Discussion and Interpretation of Viscosity

It is of interest to contrast our experimental results with viscosity data on other filled polymer systems. In Figure 9, we plot together the relative viscosity $\eta(\phi)/\eta(0)$ for the TiO_2-filled systems with data for other polymers collected from the literature. The TiO_2 data are all at the shear rate of 10 sec^{-1}. The other data are at shear rates of about 10 sec^{-1} except for the $CaSiO_3$, which is at 30 sec^{-1}. It may be seen that the relative viscosity data for the TiO_2-filled systems are generally lower than those for carbon black-rein-

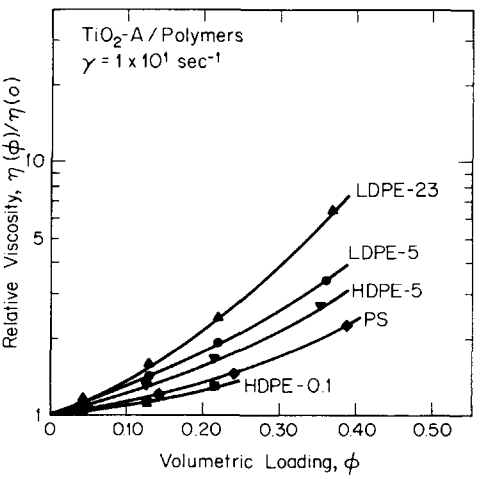

Fig. 7. Relative viscosity $\eta(\phi)/\eta(0)$ as a function of volumetric loading ϕ for the five polymers at $\dot{\gamma} = 1 \times 10^1$ sec^{-1}.

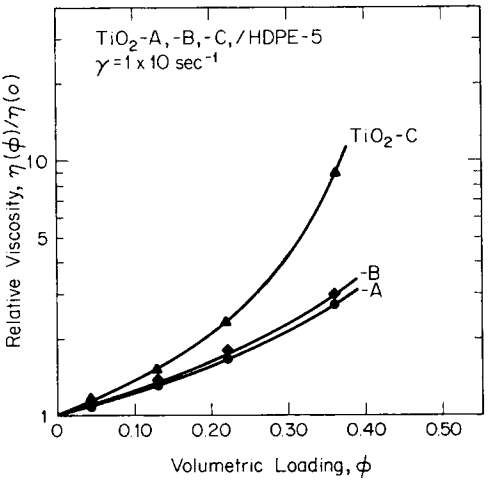

Fig. 8. Relative viscosity $\eta(\phi)/\eta(0)$ as a function of volumetric loading ϕ for HDPE-5 with different types of TiO_2.

forced elastomers. They are of the same order of magnitude as data for inorganic fillers of similar particle size. Also shown in this figure is the range of viscosity data for spheres in Newtonian liquids.[45] The increasing influence of filler content at low shear rates and the tendency toward a yield value has also been found in other filled polymer systems.[13,14,19]

The influence of the type of polymer on the extent of viscosity increase was found to be approximately reverse to the order of viscosity of polymers. One possible explanation for it is the degradation during mixing by the two-roll mill. However, this phenomenon has also been observed in filled polymer solutions[19] where degradation is unlikely, and therefore it may be characteristic of filled polymer melts as well.

We have attempted to represent the viscosity–filler loading data with a series of mathematical representations. The simplest such expression that we might use is a series of the form

$$\eta(\phi,\dot{\gamma})/\eta(0,\dot{\gamma}) = 1 + A(\dot{\gamma})\phi + B(\dot{\gamma})\phi^2 + C(\dot{\gamma})\phi^3 + \ldots . \qquad (11a)$$

Physically, A represents the hydrodynamic disturbance of the isolated particle, while B involves nearest neighbor interactions, etc. We have determined the functions A, B, and C for the polymers studied. The values decrease with increasing shear rate. At low shear rates, the parameters tend to have very large values. According to the hydrodynamic theory of the viscosity of suspensions of spheres,[43,44] A should have a value of 2.5 and B, a value near 10. This is the case at shear rates of 10^{-1} to 1 sec^{-1} in our study. These results may be physically misleading, for all experiments were carried out with reasonably large filler loadings and all of the data contain the influences of filler–filler interaction. The very large values of A, B, and C at low shear rates again suggest that the TiO_2 suspension may have a yield value.

Equation (11a) is the type of expression used to correlate dilute suspension viscosity data and is really not appropriate at the high volume loadings used

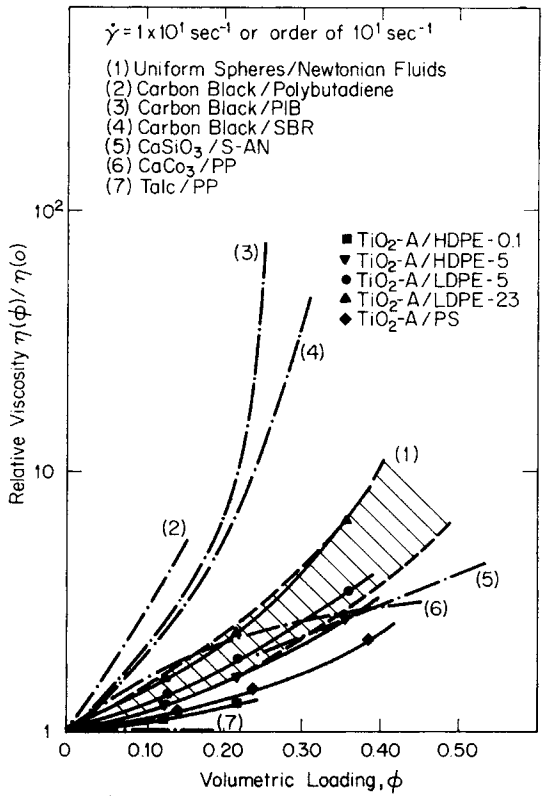

Fig. 9. Comparison of relative viscosity $\eta(\phi)/\eta(0)$ of TiO_2-filled polymer melts with data for other filled polymer melts as a function of volumetric loading ϕ.

in our study. More pertinent would be empirical equations of the Arrhenius[46] and Mooney[47] type, which have the forms

$$\ln \frac{\eta(\phi)}{\eta(0)} = a\phi \tag{11b}$$

$$\ln \frac{\eta(\phi)}{\eta(0)} = \frac{2.5\phi}{1 - c\phi}. \tag{11c}$$

For Newtonian fluids, a and c are found to have values 4.58 and 1.0 to 1.5. Plots of $\ln \eta(\phi)/\eta(0)$ versus volume fraction are shown in Figure 6, and the parameter a is plotted as a function of shear rate in Figure 9.

We now turn to the problem of the relative influence of the different types of TiO_2 on the viscosity levels of the various melts. The effects of the TiO_2-A and -B are similar, and TiO_2-C has a much greater effect on the viscosity as shown in Figure 8 and reemphasized in Figure 10, where the a parameters of eq. (11a) are compared. W. L. Dills of the du Pont Pigments Department has pointed out that the three types of TiO_2 pigments differ in method of manufacture and surface treatment. The surfaces of TiO_2-A and -B are substantially titanium dioxide, and small amounts of Al_2O_3 are contained in the crystal lattice of titanium dioxide while the surface of TiO_2-C is coated with a SiO_2–Al_2O_3 compound. The surface area of TiO_2-C pigments is almost twice as large as those of TiO_2-A and -B. The degree of aggregation is similar for

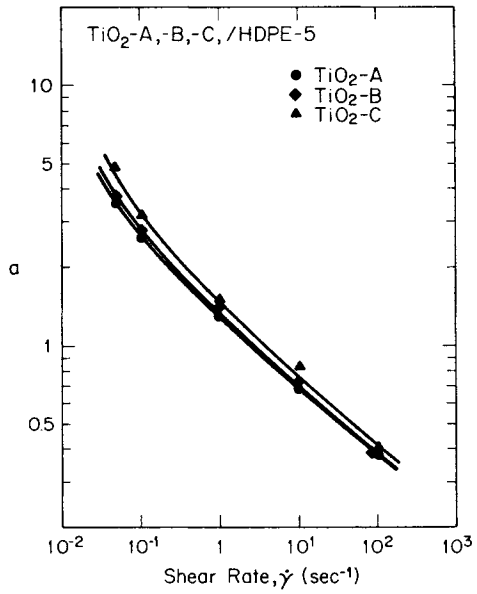

Fig. 10. Variation of a parameter of eq. (11b) as a function of shear rate $\dot{\gamma}$ for HDPE-5 with different types of TiO_2.

three types of TiO_2. Therefore, the difference of the effect of the three types on viscosity must mainly be due to the surface characteristics of the pigments, i.e., surface area and coating, which is represented by the higher oil absorption by TiO_2-C.

Normal Stress Results

The normal stress coefficient Ψ_1–shear rate $\dot{\gamma}$ relationships for the HDPE-0.1, HDPE-5, LDPE-5, LDPE-23, and PS with various loadings of TiO_2 are shown in Figures 11 and 12. It is seen that Ψ_1 is a decreasing function of shear rate at fixed loading and an increasing function of loading at fixed shear rate. As the shear rate range is rather limited, we are able to say little about the detailed interpretation of $\dot{\gamma}$ and ϕ.

Representation of Normal Stress Data

As far as the authors are aware, the normal stress data presented in this paper are the first extensive study of the influence of filler loading on this quantity. It is thus of special importance that we give some attention to the functional dependence. We have investigated two methods of correlation of the data, one based upon a Taylor series expression and a second based upon an Arrhenius type relationship. Specifically, we have considered

$$\frac{\Psi_1(\phi,\dot{\gamma})}{\Psi_1(0,\dot{\gamma})} = 1 + A'(\dot{\gamma})\phi + B'(\dot{\gamma})\phi^2 + \ldots \tag{12a}$$

$$\ln \frac{\Psi_1(\phi,\dot{\gamma})}{\Psi_1(0,\dot{\gamma})} = a'(\dot{\gamma})\phi + b'(\dot{\gamma})\phi. \tag{12b}$$

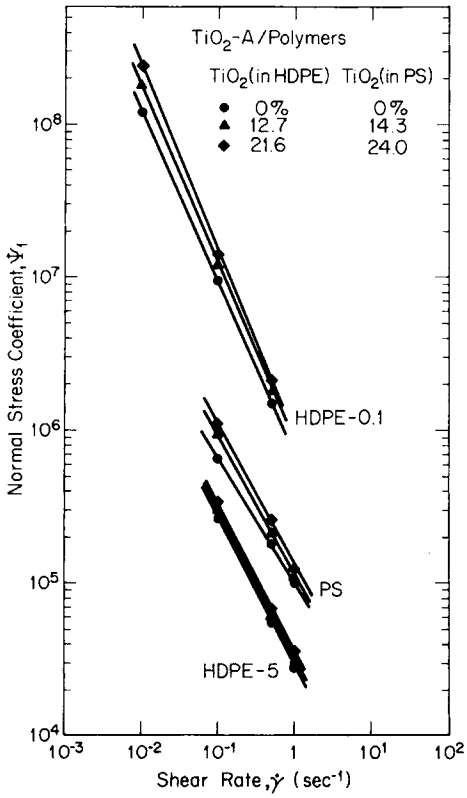

Fig. 11. Normal stress coefficient Ψ_1 as a function of shear rate $\dot{\gamma}$ for HDPE-5, HDPE-0.1, and PS with various levels of TiO_2-A.

Table IV summarizes a' and b' values for the polymer melts obtained from Figure 13, where ln $[\Psi_1(\phi,\dot{\gamma})/\Psi_1(0,\dot{\gamma})]$ is plotted against volume fraction of TiO_2. Values of A' and B' are also contained in Table IV.

Interpretation in Terms of Viscoelasticity Theory

The theory of nonlinear viscoelasticity derives relationships which connect the normal stress coefficient with the viscosity through a relaxation time $\bar{\tau}$. These expressions have the form

$$\Psi_1 = 2\bar{\tau}\eta. \tag{13}$$

TABLE IV
Constants from Eq. (12)

Polymers	A'	B'	a'	b'
HDPE-0.1	1.2	1.1	0.56	0.20
HDPE-5	0.60	1.2	0.32	0.55
LDPE-5	2.0	11	1.2	3.9
LDPE-23	4.6	35	2.3	5.5
PS	0.90	3.5	0.48	0.70

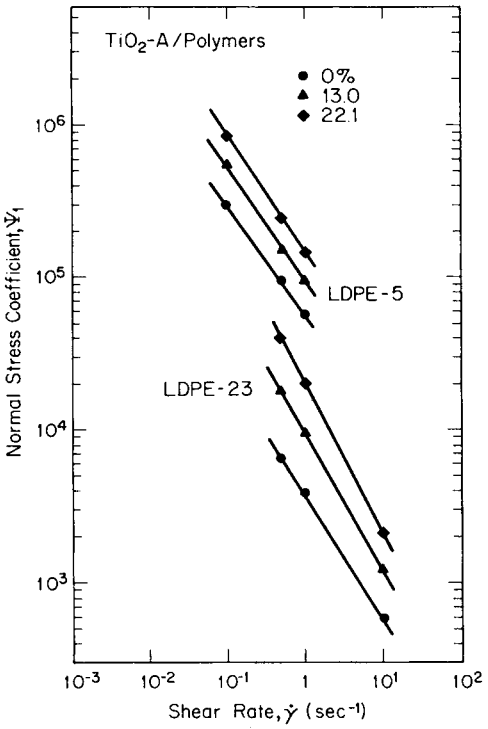

Fig. 12. Normal stress coefficient Ψ_1 as a function of shear rate $\dot{\gamma}$ for LDPE-5 and LDPE-23 with various levels of TiO_2-A.

According to the work of Coleman and Markovitz[48] we have for the second order fluid which is a "slow flow" asymptote

$$\lim_{\dot{\gamma}\to 0} \frac{\Psi_1}{2\eta} = \bar{\tau} = \frac{\int_0^\infty sG(s)ds}{\int_0^\infty G(s)ds} \tag{14}$$

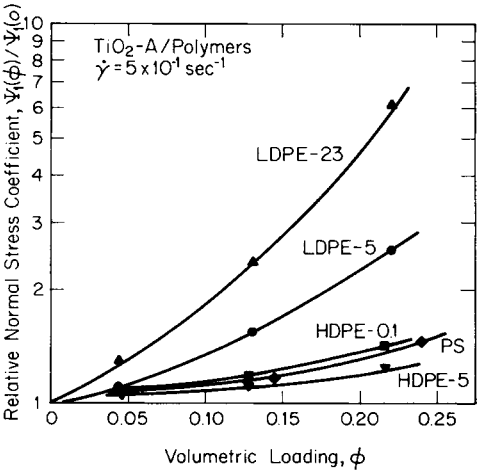

Fig. 13. Relative normal stress coefficient $\Psi_1(\phi)/\Psi_1(0)$ as a function of volumetric loading ϕ for five polymers with TiO_2-A at $\dot{\gamma} = 5 \times 10^{-1}$ sec^{-1}.

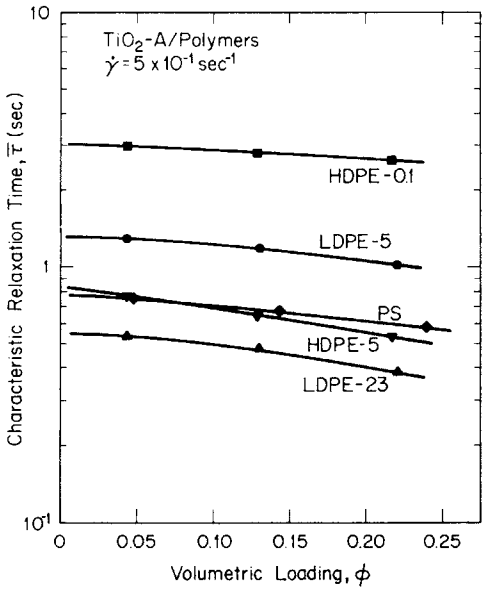

Fig. 14. Characteristic relaxation time $\bar{\tau}$ as a function of volumetric loading ϕ for five polymers with TiO_2-A.

where $G(s)$ is the relaxation modulus of linear viscoelasticity. The Bogue-White theory,[49,50] which is useful in a higher shear rate range, predicts

$$\frac{\Psi_1}{2\eta} = \bar{\tau} = \frac{\Sigma G_i \tau^2_{\text{ieff}}}{\Sigma G_i \tau_{\text{ieff}}} \tag{15}$$

where τ_{ieff} are deformation rate-dependent relaxation times. Other constitutive equations lead to similar relationships. One must proceed with caution, however, in applying traditional viscoelasticity theory to filled melts, as these systems exhibit yield values and may be thixotropic.[4]

In Figure 14, we have plotted the characteristic relaxation time $\bar{\tau}$ determined from eq. (13) as a function of volume loading. It is clear that increasing ϕ decreases $\bar{\tau}$.

We have expressed $\bar{\tau}$ in the forms

$$\frac{\bar{\tau}(\phi,\dot{\gamma})}{\bar{\tau}(0,\dot{\gamma})} = 1 + A''(\dot{\gamma})\phi + B''(\dot{\gamma})\phi^2 + \ldots \tag{16a}$$

$$\ln \frac{\bar{\tau}(\phi,\dot{\gamma})}{\bar{\tau}(0,\dot{\gamma})} = a''(\dot{\gamma})\phi + b''(\dot{\gamma})\phi^2. \tag{16b}$$

The values of A'', B'', a'', and b'' are summarized in Table V.

The above results are the first study of a characteristic relaxation time of filled polymer melts determined from normal stress data. Our conclusions are in agreement with the earlier studies of Vinogradov et al.,[11] Han,[15] and White and Crowder[12] that the addition of filler tends to reduce the elastic memory of polymer melts. We would suggest that the recent study of Matsumoto, Hitomi, and Onogi,[25] which suggests a higher maximum relaxation time in carbon black-filled polymer solutions, using linear viscoelastic low-

TABLE V
Constants from Eq. (16)

Polymers	A''	B''	a''	b''
HDPE-0.1	−0.41	−1.1	−0.28	0
HDPE-5	−1.5	−2.1	−0.80	−1.3
LDPE-5	−0.44	−1.0	−0.30	−0.84
LDPE-23	−0.68	−1.3	−0.42	−1.3
PS	−0.80	−0.74	−0.77	0

frequency dynamic measurements, is really determining the existence of a near yield value. These results are not pertinent at moderate and high shear rates.

EXTRUSION

Extrudate Swell Results

In Figures 15–20, we plot the variation of frozen and annealed extrudate swell $B(= d/D)$ with L/D ratio at fixed shear rate and with shear rate at fixed large L/D ratio (L/D = 28) for the polmer melts studied with various TiO_2 loadings. It is clear that extrudate swell decreases with L/D ratio and in-

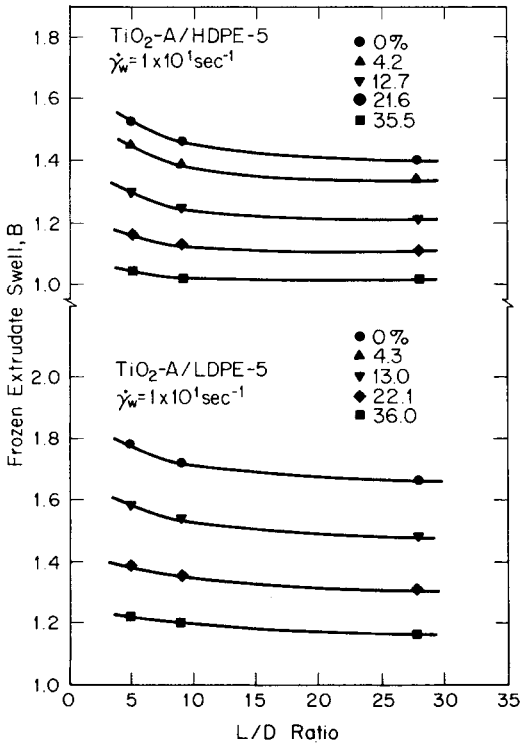

Fig. 15. Frozen extrudate swell B as a function of L/D ratio for the HDPE-5 and the LDPE-5 with different TiO_2 loading.

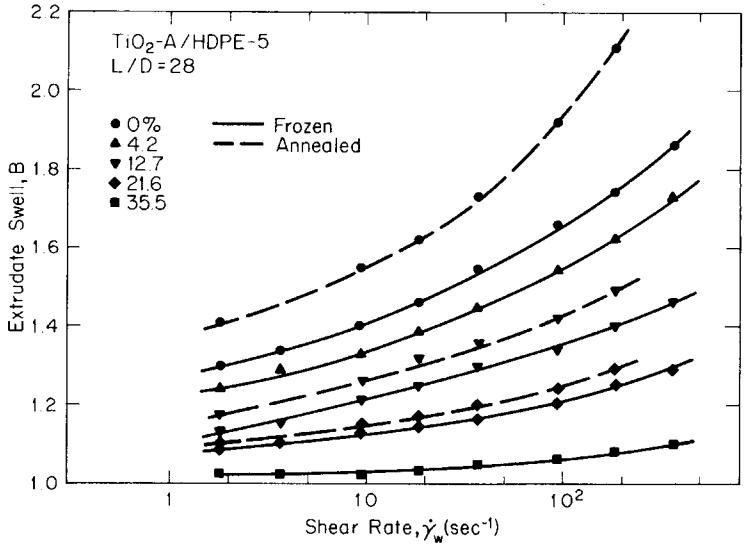

Fig. 16. Frozen and annealed extrudate swell B of HDPE-5 with TiO_2-A as a function of capillary wall shear rate $\dot{\gamma}_w$ at L/D 28.

creases with shear rate. The presence of TiO_2 filler decreases the extrudate swell, with increasing levels of TiO_2 causing further decreases. This is emphasized in Figure 21, where we plot extrudate swell as a function of volume fraction of filler at fixed L/D ratio (= 28) and shear rate. The influence of annealing in hot silicone oil is shown in Figures 16–20. Clearly, the influence of the TiO_2 is to decrease the recovery of extrudates.

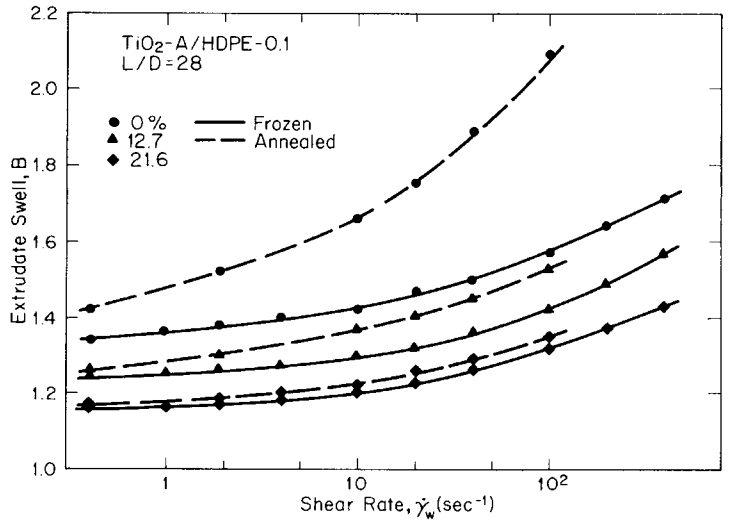

Fig. 17. Frozen and annealed extrudate swell B of HDPE-0.1 with TiO_2-A as a function of capillary wall shear rate $\dot{\gamma}_w$ at L/D = 28.

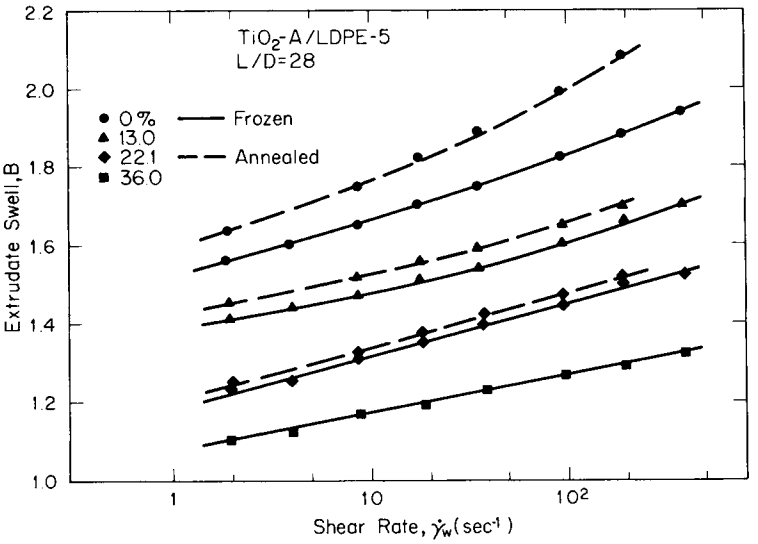

Fig. 18. Frozen and annealed extrudate swell B of LDPE-5 with TiO_2-A as a function of capillary wall shear rate $\dot{\gamma}_w$ at $L/D = 28$.

Interpretation of Extrudate Swell

Extrudate swell has long been realized to have its origins in unconstrained elastic recovery following Poiseuille flow.[36,51–54] The only reasonable interpretation of the extrudate swell data is that its decrease is due to decreased elastic memory of the filled melts. The reduction in $\bar{\tau}$ and in further recovery of the extrudate by annealing supports this view. The same idea has been expressed earlier by Vinogradov et al.[11] and White and Crowder.[12]

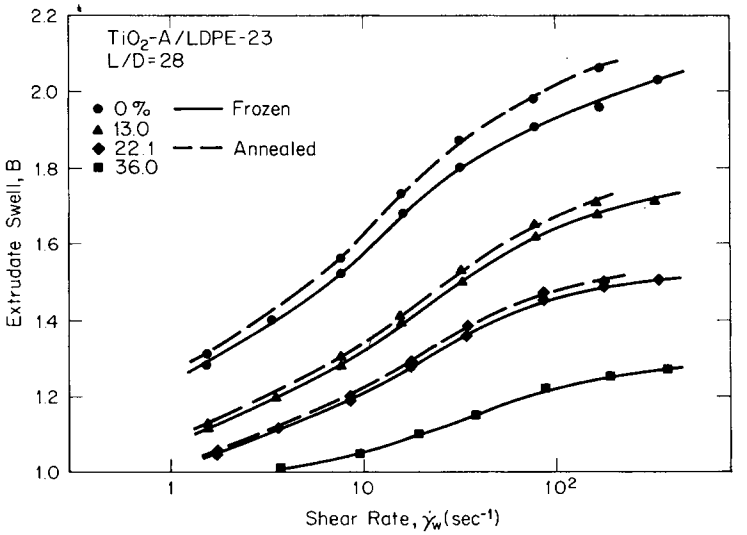

Fig. 19. Frozen and annealed extrudate swell B of LDPE23 with TiO_2-A as a function of capillary wall shear rate $\dot{\gamma}_w$ at $L/D = 28$.

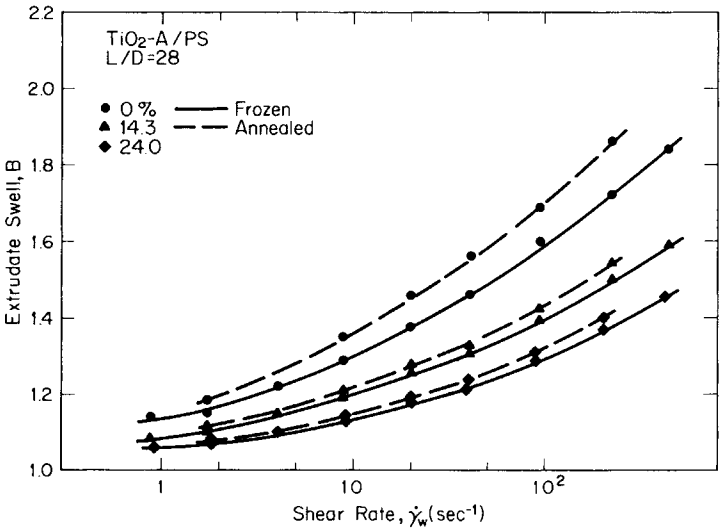

Fig. 20. Frozen and annealed extrudate swell B of PS with TiO_2-A as a function of capillary wall shear rate $\dot{\gamma}_w$ at $L/D = 28$.

Newman and Trementozzi[13] attempted to explain the decrease in extrudate swell with addition of filler through (1) volume fraction effects, (2) increase in modulus due to presence of filler, (3) velocity profile, and (4) migration of filler particles. Mechanisms (1) and (2) are certainly part of the influence of filler on phenomenological viscoelastic properties. Point (3) is certainly true, but its effect is clearly minor. The influence of mechanism (4) is obscure.

Let us examine extrudate swell from the view of viscoelasticity theory. From dimensional analysis of the equations of motion for creeping flow of a viscoelastic fluid, it may be shown that the extrudate swell is given by[39,49,50,55]

$$B = F\left[\bar{\tau}\frac{V}{D}, \text{viscoelastic ratio numbers}, \frac{L}{D}, \text{entrance geometry}\right] \quad (17)$$

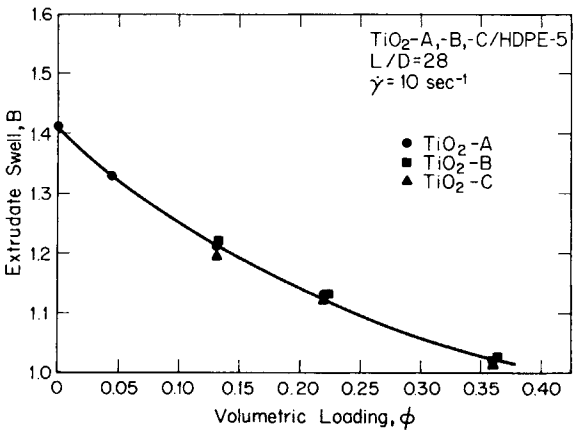

Fig. 21. Frozen extrudate swell B of HDPE-5 as a function of volumetric loading ϕ at $L/D = 28$ and $\dot{\gamma}_w = 1 \times 10^1$ sec^{-1}.

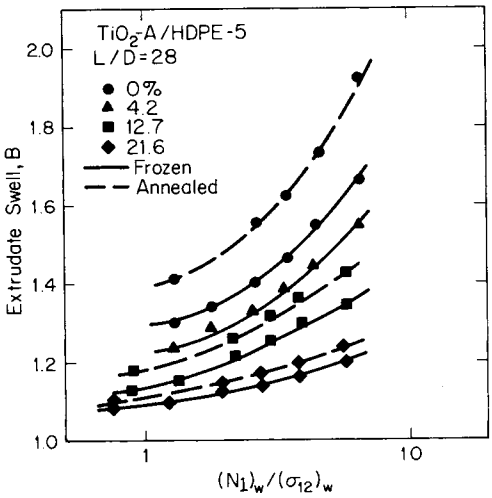

Fig. 22. Frozen and annealed extrudate swell B of HDPE-5 with TiO_2-A as a function of $(N_1)_w/(\sigma_{12})_w$ at $L/D = 28$.

where $\bar{\tau}\ V/D$ is a Weissenberg number. Clearly, for large L/D, B should be correlated with $\bar{\tau}\ V/D$, which from eqs. (7a) and (14) is proportional to $(N_1)_w/(\sigma_{12})_w$ where the subscript w refers to the die swell.

Figure 22 plots frozen extrudate swell for the HDPE-5-TiO_2 system as a function of $(N_1)_w/(\sigma_{12})_w$ for the longest die ($L/D = 28$). The agreement is not good. If we compare the annealed rather than the frozen extrudate data, the scatter is worse. It should be clear that the influence of filler on extrudate swell is greater than on relaxation time. At fixed $(N_1)_w/(\sigma_{12})_w$ or $\bar{\tau}\ \dot{\gamma}_w$, the value of B decreases with increasing filler content. Various reasons may exist for the discrepancy. First, filled melts exhibit yield values as we have seen and have been characterized as thixotropic.[4] Their constitutive equations are undoubtedly very different. At a minimum, the viscoelastic ratio numbers of eq. (17) should be considered. A second reason is that an L/D of 28 is not equivalent to an infinite L/D ratio, and we are overestimating B for the unfilled and lightly filled melts.

Figures 23a and 23b plot B as a function of $(N_1)_w/(\sigma_{12})_w$ with data limited to a fixed value of $(\sigma_{12})_w$. The agreement is good. The reason for this is unclear.

Extrudate Distortion

At high extrusion rates, the extrudates of unfilled molten polymers all become distorted. The extrusion rate or shear rate range at which this distortion occurs is characteristic of the system, as is the detailed shape of the extrudate. Generally, the influence of addition of TiO_2 is to smoothen the surface of extrudates and to delay the occurrence of extrudate distortion until higher extrusion rates. This point is made in Figure 24, where we plot the capillary wall shear rate and shear stress at which distortion occurs as a function of TiO_2 loading.

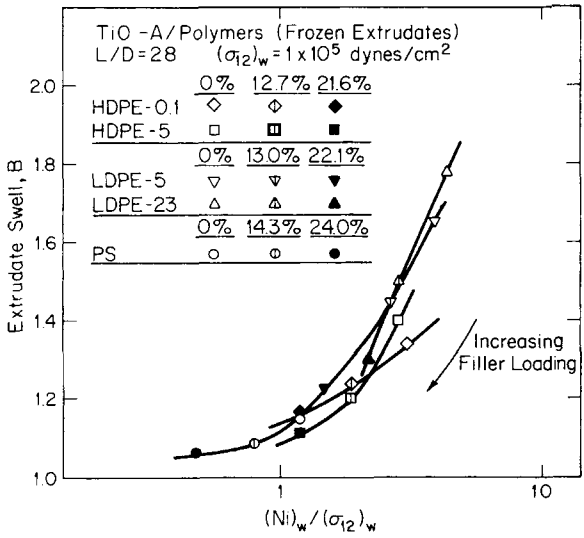

(a)

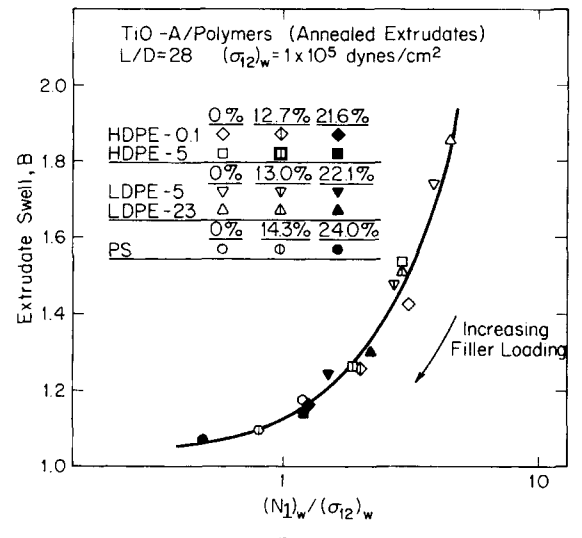

(b)

Fig. 23. (a) Frozen extrudate swell B of five polymers with TiO_2-A as a function of $(N_1)_w/(\sigma_{12})_w$ at $L/D = 28$ and $(\sigma_{12})_w = 1 \times 10^5$ dyne/cm^2. (b) Annealed extrudate swell B of five polymers with TiO_2-A as a function of $(N_1)_w/(\sigma_{12})_w$ at $L/D = 28$ and $(\sigma_{12})_w = 1 \times 10^5$ dyne/cm^2.

Our observations on the onset of extrudate distortion are in general agreement with earlier workers. The shape of the distorted extrudates of unfilled melts are similar to those described earlier.[29,56,57] The finding that carbon black retards the extrudate distortion in rubber is well known,[6,11,12] and its significance is discussed by White and Crowder.[12] The effect seems generally associated with the decrease in melt elasticity and extrudate swell which occurs with the addition of filler.

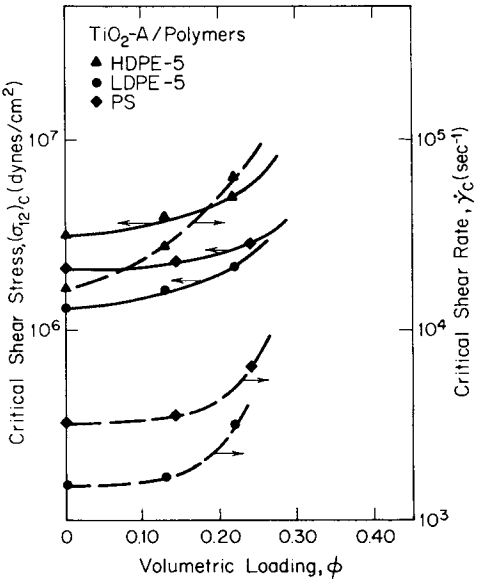

Fig. 24. Critical shear stress $(\sigma_{12})_c$ and critical shear rate $\dot{\gamma}_c$ at the onset of extrudate distoration as a function of volumetric loading ϕ.

Entrance Pressure Loss

The influence of filler loading on the entrance pressure loss Δp_e was determined. It was found that the TiO_2 has little influence on $\Delta p_e/(\sigma_{12})_2$. It should be noted that the above observations are not in agreement with the earlier work of Bagley[17] and White and Crowder[12] who found this ratio to be decreased by filler addition.

However, there may be another explanation. The total pressure drop in an Instron capillary rheometer is actually composed of three terms:

$$p = \Delta p_e + \Delta p_c + \Delta p_b = \Delta p_e + 4(\sigma_{12})_w \left(\frac{L}{D}\right) + 4(\sigma_{12})_{bw} \left(\frac{L}{D}\right)_b \qquad (19)$$

where Δp_e is the pressure drop at the entrance and exits of the die; Δp_c, in the capillary; and Δp_b, in a barrel.[58] This last term is generally neglected because of its small magnitude. However, with the polymer melts having a tendency to exhibit yield value, the shear stress at low shear rates in the barrel $(\sigma_{12})_{bw}$ equals the yield value, and Δp_b may not be negligible. The extra pressure drop measurement is the sum of Δp_e and Δp_b. As Δp_b increases with filler loading at fixed shear rate and the difference $p - \Delta p_c$ remains unchanged, we may actually have Δp_e decreasing with filler loading. The response will vary depending upon the relative reduction in elasticity and tendency towards a yield value. It should be added that, as pointed out by Han,[59] Δp_e determined from the Bagley plot is a rather complex quantity if the exit pressure loss varies with L/D. However, this should not alter the thrust of the above discussion.

The authors would like to thank Phillips Petroleum, Dow Chemical, and Union Carbide for supplying the polymers used in this study. E. I. du Pont de Nemours supplied the TiO_2 used in this study. Dr. W. L. Dills of du Pont was very helpful throughout the course of this study in supplying information and answering queries on TiO_2.

References

1. M. Londergan and W. F. Spengeman, *J. Paint. Technol.*, **42**, 266 (1970).
2. R. H. Zabel, paper presented at Rochester Regional Conference, Society of Plastics Engineers, April 1962.
3. W. D. Ross, *Ind. Eng. Chem., Prod. Res. Develop.*, **13**, 45 (1974).
4. L. Mullins, *J. Phys. Coll. Chem.*, **54**, 239 (1950); L. Mullins and R. W. Whorlow, *Trans. IRI*, **27**, 55 (1951).
5. C. C. McCabe and N. Mueller, *Trans. Soc. Rheol.*, **5**, 329 (1961).
6. N. V. Zakharenko, F. S. Tolstukhina, and G. M. Bartenev, *Rubber Chem. Technol.*, **35**, 326 (1962).
7. J. R. Hopper, *Rubber Chem. Technol.*, **40**, 463 (1967).
8. P. P. A. Smit, *Rheol. Acta*, **8**, 277 (1969); P. P. A. Smit and A. K. van der Vegt, *Kautschuk und Gummi;* **23** (4), 147 (1970).
9. E. A. Collins and J. T. Oetzel, *Rubber Age*, **102**, 64 (1970).
10. T. Matsumoto, A. Takashima, T. Masuda, and S. Onogi, *Trans. Soc. Rheol.*, **14**, 617 (1970).
11. G. V. Vinogradov, A. Y. Malkin, E. P. Plotnikova, O. Y. Sabsai, and N. E. Nikolayeva, *Int. J. Polym. Mat.*, **2**, 1 (1972).
12. J. L. White and J. W. Crowder, *J. Appl. Polym. Sci.*, **18**, 1013 (1974).
13. S. Newman and Q. A. Trementozzi, *J. Appl. Polym. Sci.*, **9**, 3071 (1965).
14. F. M. Chapman and T. S. Lee, *S.P.E. J.*, **26**, (1), 37 (1970).
15. C. D. Han, *J. Appl. Polym. Sci.*, **18**, 821 (1974).
16. S. Onogi, T. Matsumoto, and Y. Warashina, *Trans. Soc. Rheol.*, **17**, 175 (1972).
17. E. B. Bagley, paper presented at the Society of Rheology Meeting, St. Paul, Minnesota, October 1969.
18. F. Nazem and C. T. Hill, *Trans. Soc. Rheol.*, **18**, 87 (1974).
19. L. Nicodemo and L. Nicolais, *J. Appl. Polym. Sci.*, **18**, 2539 (1974).
20. J. S. Chong, E. B. Christiansen, and A. D. Baer, *J. Appl. Polym. Sci.*, **15**, 2007 (1971).
21. R. F. Landel, *Trans. Soc. Rheol.*, **2**, 53 (1958).
22. H. Kambe and M. Tanaka, *Proc. 4th Int. Rheol. Congr.*, **3**, 557 (1965).
23. S. Onogi, T. Masuda, and T. Matsumoto, *Trans. Soc. Rheol.*, **14**, 275 (1970).
24. H. Kumatsu, T. Mitsui, and S. Onogi, *Trans. Soc. Rheol.*, **17**, 351 (1973).
25. T. Matsumoto, C. Hitomi, and S. Onogi, *J. Soc. Rheol. Japan*, **2**, 12 (1974).
26. W. F. O. Pollett, *Brit. J. Appl. Phys.*, **6**, 199 (1955).
27. R. G. King, *Rheol. Acta*, **5**, 35 (1966).
28. K. Sakamoto, N. Ishida, and Y. Fukasawa, *J. Polym. Sci. A-2*, **6**, 1999 (1968); K. Sakamoto and R. S. Porter, *J. Polym. Sci. B*, **8**, 177 (1970).
29. T. F. Ballenger, I. J. Chen, G. E. Hagler, D. C. Bogue, and J. L. White, *Trans. Soc. Rheol.*, **15**, 195 (1971).
30. C. D. Han, K. U. Kim, N. Siskovic, and C. R. Huang, *J. Appl. Polym. Sci.*, **17**, 95 (1973).
31. B. L. Lee and J. L. White, *Trans. Soc. Rheol.*, **18**, 467 (1974).
32. S. M. Freeman and K. Weissenberg, *Nature*, **161**, 324 (1948).
33. S. Middleman, *The Flow of High Polymers*, Wiley, New York, 1968.
34. R. Eisenschitz, B. Rabinowitsch and K. Weissenberg, *Mitt. Deut. Mat.*, **9**, 91 (1929); B. Rabinowitsch, *Z. Phys. Chem.*, **A145**, 1 (1929); R. Eisenchitz, *Kolloid-Z.*, **59**, 184 (1933).
35. E. B. Bagley, *J. Appl. Phys.*, **28**, 624 (1957).
36. N. Nakajima and M. Shida, *Trans. Soc. Rheol.*, **10**, 299 (1966).
37. R. A. Mendelson, F. L. Finger, and E. B. Bagley, *J. Polym. Sci.*, **C35**, 177 (1971).
38. R. A. Mendelson and F. L. Finger, *J. Appl. Polym. Sci.*, **17**, 797 (1973).
39. J. L. White and J. F. Roman, University of Tennessee Polymer Science and Engineering Report #36, January 1975; *J. Appl. Polym. Sci.*, in press.
40. W. Philippoff and F. H. Gaskins, *Trans. Soc. Rheol.*, **2**, 263 (1958).
41. H. L. LaNieve and D. C. Bogue, *J. Appl. Polym. Sci.*, **12**, 353 (1968).
42. T. F. Ballenger, and J. L. White, *J. Appl. Polym. Sci.*, **15**, 1949 (1971).
43. A. Einstein, *Ann. Phys.*, **19**, 289 (1906); *ibid.*, **34**, 591 (1911), republished in translation in *The Theory of Brownian Movement*, Dover, New York, 1956.
44. J. Happel and H. Brenner, *Low Reynolds Number Hydrodynamics*, Prentice-Hall, Englewood Cliffs 1965.

45. D. G. Thomas, *J. Colloid Sci.*, **20,** 267 (1965).
46. S. Arrhenius, *Z. Phys. Chem.*, **1,** 285 (1887).
47. M. Mooney, *J. Colloid, Sci.*, **6,** 162 (1951).
48. B. D. Coleman and H. Markovitz, *J. Appl. Phys.*, **35,** 1 (1964).
49. D. C. Bogue and J. L. White, Engineering Analysis of Non-Newtonian Fluids, NATO Agardograph No. 144, 1970.
50. I. J. Chen and D. C. Bogue, *Trans. Soc. Rheol.*, **16,** 59 (1972).
51. J. L. White, *Trans. Soc. Rheol.*, **19,** 271 (1975).
52. J. H. Dillon and N. Johnston, *Physics*, **4,** 225 (1933).
53. R. S. Spencer and R. E. Dillon, *J. Colloid Sci.*, **3,** 163 (1948).
54. E. B. Bagley, S. H. Storey, and D. C. West, *J. Appl. Polym. Sci.*, **7,** 1661 (1963).
55. A. B. Metzner, J. L. White, and M. M. Denn, *AIChE J.*, **12,** 863 (1966); J. L. White and N. Tokita, *J. Appl. Polym. Sci.*, **11,** 321 (1967).
56. J. P. Tordella, *J. Appl. Phys.*, **27,** 454 (1956); *Rheol. Acta*, 1 216 (1958); *J. Appl. Polym. Sci.*, **7,** 215 (1963).
57. J. L. White, *Appl. Polym. Symp.*, **20,** 155 (1973).
58. A. P. Metzger and J. R. Knox, *Trans. Soc. Rheol.*, **9,** 13 (1965).
59. C. D. Han, *Trans. Soc. Rheol.*, **17,** 375 (1973).

Received February 11, 1975
Revised June 2, 1975